Proceedings of the
Annual Stability Conference
Structural Stability Research Council
Louisville, Kentucky, April 1-4, 2025

Experimental and analytical stability of thick origami panels for deployable anchors to prevent coastal erosion

Elizabeth Capretta[1], Khuzaima Hummad[2], Ann C. Sychterz[3]

Abstract
Underground anchors are often large and heavy due to being over-designed, and this results in expensive transportation costs that consume significant amounts of fuel. Underground deployable anchors offer materially efficient alternatives that can address the growing challenge of slope instability in coastal areas exacerbated by shifting climates. A novel design for deployable ground anchors consists of a pile with deployable attachments, referred to as awns. This design uses less material to achieve an equivalent surface area when compared to cylindrical piles. The installation process for deployable ground anchors is torque-driven, like that of drilled shafts, rather than using impact or vibration hammers. This paper presents an experimental methodology to determine the increase in the shear plane in sandy soil using deployable underground anchors. Ink dots were placed on the bottom of a test box, where a document camera captured the movement of the ink dots, and an ink tracking technique was employed to locate the shear plane. In addition to experimentally assessing the performance of the ground anchors, a computational analysis is completed by creating an equivalent bar and hinge model of the awns, considering both in-plane and out-of-plane loading scenarios. The findings of this study are that the ink tracking technique in sandy soil is useful for experimentally determining the shear plane effects of deployable awns from the ground anchor, and that the bar cross-section optimization adequately represents the behavior of thick origami as it pertains to the deployable awns under in-plane and out-of-plane loading. These insights are significant advancements for understanding the optimal design and functionality of deployable ground anchors.

1. Introduction

Coastal communities bordering the Great Lakes contend with the persistent challenge of bluff instability, which is attributable to the fluctuating water levels of the lakes. This challenge can cause considerable and often expensive effects on infrastructure, public and private properties, and environmental habitats (Volpano et al. 2020, Lawrence 1994). Coastlines along the Great Lakes are often interwoven with the collective identity of the respective coastal communities (Levine et al. 2020). Thus, there is a need to develop a slope stabilization method that mitigates the adverse effects on the coastline while preserving the community's engagement with this geographical feature.

[1] Graduate Research Assistant, University of Illinois Urbana-Champaign, <ec36@illinois.edu>
[2] Graduate Research Assistant, University of Illinois Urbana-Champaign, <khummad2@illinois.edu>
[3] Assistant Professor, University of Illinois Urbana-Champaign, <asychter@illinois.edu>

Traditional cylindrical reinforcing piles have been designed and used for stabilizing steep slopes (Poulos 1995). These piles are conventionally designed based on the pile's surface area interacting with the soil, as this interaction determines the pull-out capacity (Aubeny 2017). Consequently, cylindrical piles tend to be over-designed, using more material than strictly necessary to meet strength requirements. The installation of underground piles, typically through using impact or vibration hammers, induces vibrations in the surrounding soil, and poses potential harm to nearby existing structures or equipment (Colaço et al. 2021). To address these challenges, this laboratory has developed a deployable structure, aiming to be a materially efficient design that has less significant effects on nearby structures. This novel design features a pile with deployable attachments, referred to as awns. This design can maintain an equivalent surface area to cylindrical piles while using less material due to the deployable awn attachments. Furthermore, this design utilizes a torque-driven installation process, similar to the installation process for drilled shafts, rather than using impact or vibration hammers. The shear plane effects of these deployable awns in sandy soil have yet to be experimentally explored, and an equivalent model of these awns has yet to be computationally analyzed.

Within the field of geotechnical engineering, there have been studies that explore geotechnical systems that deploy during installation such as suction embedded plate anchors (SEPLAs) and piles with anchor wings (Wilde et al. 2001, Aubeny 2017, Sakr et al. 2020). Concurrently, experimental investigations have explored the effects of soil disturbance during the installation of helical piles on their tensile capacity (Lutenegger and Tsuha 2015). Large scale tests have also been performed to study the soil disturbance effects associated with the drilling of tie back anchors (Kempfert and Gebreselassie 1999, Lande et al. 2020). However, an analysis of the shear plane in sandy soil, resulting from the installation of the deployable ground anchor, remains unexplored.

Origami structures have successfully been modeled using bar-and-hinge models (Filipov et al. 2017). Previous work in this lab has modeled origami as bar-and-hinge models by modeling the creases as hinges and the panels in between the creases as rigid links (Sychterz and Baruah 2021, Baruah and Sychterz 2022). Bar-and-hinge models have yet to be used for modeling the deployable awn attachments on underground deployable anchors.

The first objective of this paper is to develop an ink tracking technique that successfully defines the shear plane location that results from the deployment of underground deployable anchors. The second objective of this paper is to model the deployable awn attachments as bar-and-hinge models.

2. Procedures

2.1 Shear Plane Test Set Up

A setup was constructed to deploy the anchor while recording the sand displacement data. A representation of the test set up can be seen in Figure 1. A similar test set up was used previously in this lab, using the same materials (Tucker and Sychterz 2022). A clear acrylic box with dimensions 5-3/4" x 5-3/4" x 1-7/8" sat on an elevated wooden crate. Below the crate was a document camera to capture the bottom of the box acrylic box as the anchor was deployed. Two pieces of wood were clamped beside to the acrylic box to prevent the box from shifting during the tests. Pulley clamps were attached to the edges of the crate and were aligned with the center of the acrylic box.

Gel food coloring was mixed with water in a 1:1 ratio to create a concentrated ink mixture. The ink was added to the bottom of the acrylic box as dots in a grid pattern, at a spacing of ¼", as shown in Figure 1b. The deployable anchor was placed in the center of the acrylic box with a 1 mm thick layer of petroleum jelly under the pile of the anchor. A prototype ground anchor was 3D printed. The pile of the ground anchor has a diameter of 25 mm and a height of 75mm and was printed with the material, VeroMagentaV. The awns of the ground anchor had a height of 25 mm, and the thickness of the awn is tapered to the circumference of the anchor, with the largest thickness being 2 mm. The material of the 3D-printed awns was a mix of VeroMagenta and Agilus. The petroleum jelly helped keep the deployable anchor in place during the test set up, and to ensure that the anchor deployed smoothly without sand underneath the pile.

Once the ink pattern was added to the bottom of the acrylic box and the anchor was placed in the center of the box, fused silica sand was added into the acrylic box up to a 25 mm mark to ensure the awns were covered. An acrylic lid with a hole cut out for the pile of the deployable anchor was placed near the top of the acrylic box to ensure that the anchor maintained its position at the center of the box during the test, and to allow for sand to move over the awns as they deployed. Next, a nylon string was threaded through the hole in the top of the pile of the ground anchor, wrapped in the counterclockwise direction around the top of the pile, and then laid across the pulleys on the sides of the wooden crate and tied together underneath the table. During the test, the nylon cord is pulled to deploy the anchor 180 degrees. A force sensor was attached to the nylon cord beneath the table to record the applied force. Additionally, 10 N weight was placed on top of the ground anchor to ensure the deployable anchor did not lift out of the acrylic box during the test.

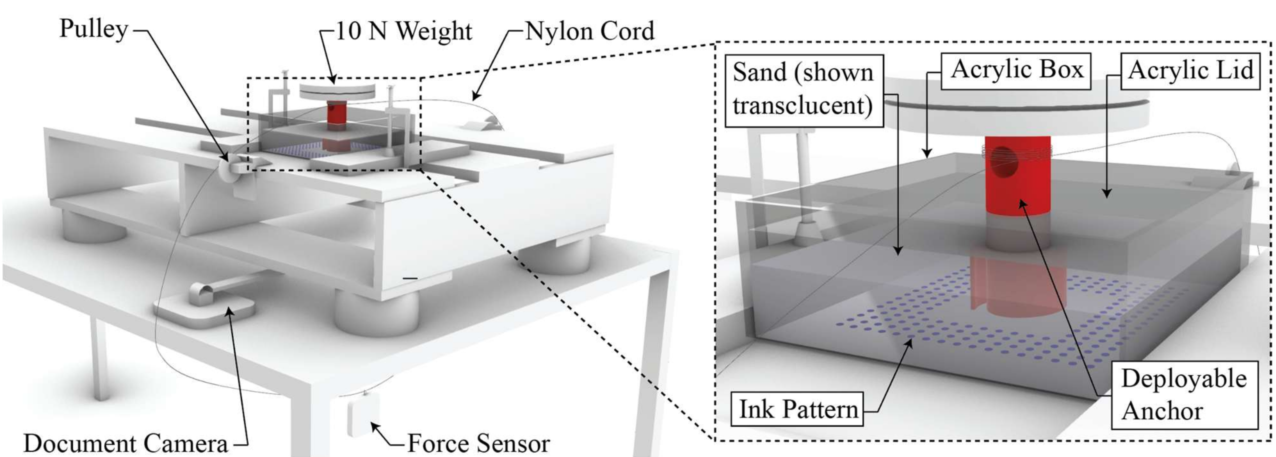

(a) Data collection

(b) Deployable anchor box set up

Figure 1. Test set up configuration with (a) data collection of video and force and (b) ink-tracking.

2.2 Ink Tracking Technique

The movement of the ink pattern on the bottom of the test set up box is recorded by the document camera beneath the box during deployment. The displacement of the ink dots is used to determine the location of the shear plane that results from the deployment of the awns. The methodology that is developed is described in the results section of this paper.

2.3 Bar and Hinge Model Creation Procedure

To analyze the structural behavior of a single awn, an equivalent representation of the awn was created in the form of a bar and hinge truss model (Figure 2). By matching the deformations of the bar and hinge model to the deformation of the awn, the model was created. This model is developed to represent the awns protruding from the pile to quantify the in-plane and out-of-plane deformation behavior. Figure 3 describes the detailed steps for the creation of this model. Initially, the awns are analyzed to calculate the in-plane and out-of-plane deformations when loads are applied with pinned and roller boundary conditions. The loads are distributed across the end node. To form the bar and hinge model, the bar elements are sized to match the overall geometry of the awn plate so that the bar model has the same planar dimensions as the awn (25 mm x 25 mm). To determine the individual bar diameters, the total volume in the awn plate is equated to the combined volume in all the circular bars, by $D_b = 2\sqrt{\frac{V_a}{\pi L_b}}$, where D_b is the new bar diameter, V_a is the volume of the awn, and L_b is the length of the bars. This establishes an initial proportional size estimate across the various truss elements.

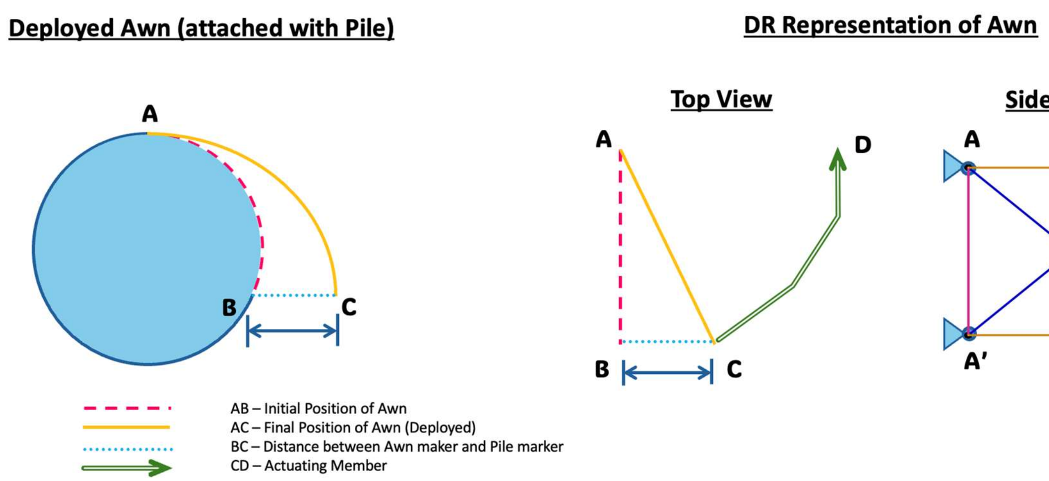

Figure 2. (a) Deployed awn (attached with pile) (b) Dynamic relaxation representation of awn, top view. (c) Dynamic relaxation representation of awn, side view

With the initial bar model established, the out-of-plane deformations under loading are calculated and compared to the awn deformations. If the bar deformation results are within 10% error of the awn, they are considered acceptable. If the error margin exceeds 10%, the stiffness of the bars is modified by adjusting their diameter. Adjustments to the diameter are completed using the procedure in Figure 4. A multiplier ratio is found and used to alter the bar diameters to better match the stiffness of the awn. The out-of-plane deformation with the new diameter is re-calculated and compared to the experimental awn deformation. Using the tuned diameters from the out-of-plane analysis, the bar model is further assessed for in-plane deformations. Both the longitudinal and lateral axial deformations are quantified under loading. These results are compared to the awn deformation. If the bar-in-plane deformations match within 10% error margin, the model sufficiently represents an equivalent simulation of the awn. If deviations exceed 10%, the iterative diameter tuning process shown in Figure 3 is repeated, and the iteration repeats until there is a deformation of the bar-and-hinge model within 10% error of the deformation of the awn.

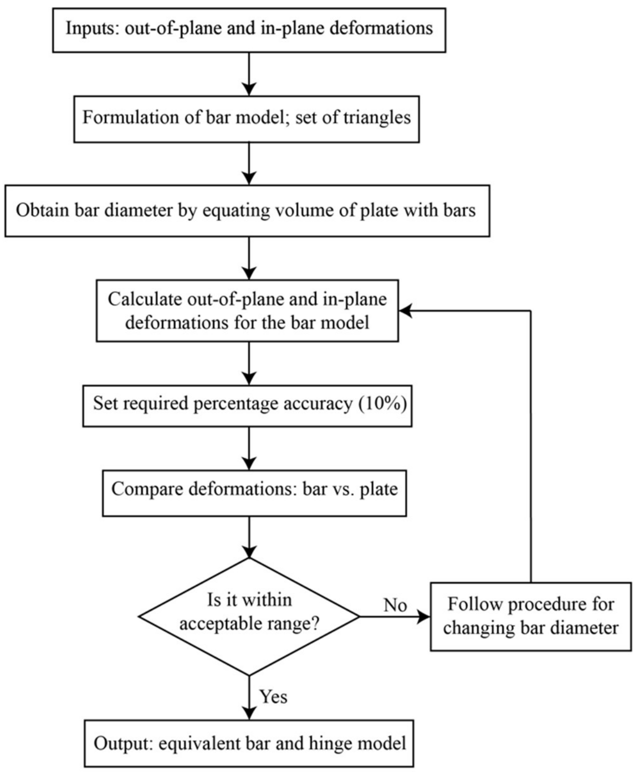

Figure 3. Overview of Bar-and-Hinge Model Creation

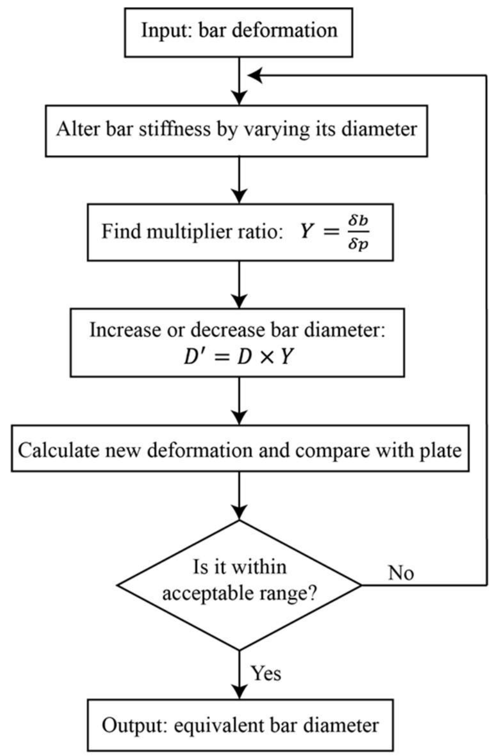

Figure 4. Procedure for Changing Bar Diameter

3. Results

3.1 Ink Tracking Technique

To find the shear plane location due to the deployment of the ground anchor, an ink spread tracking technique was developed. First, two images must be taken from the recording of the deployment test. The first image is the initial configuration before deployment, Figure 5a, and the second image is the final configuration after the deployment of the ground anchor, Figure 5b. The initial configuration image is overlaid on the final configuration to create the overlay image that will be analyzed, Figure 5c.

The overlay image is imported to Rhino3D and analyzed using a Grasshopper code. First, the displacement of the pile is found, which will help determine the lower threshold of the displacement of the ink dots. If the displacement of the pile is significant (larger than 0.5 mm), then the minimum threshold for the displacement of the ink dots will be half the displacement of the pile. If the displacement of the pile is not significant (less than 0.5 mm) then the value for the minimum threshold of the displacement of the ink dots is 0.5 mm. The image is then divided into eight sections, and the displacement of the ink dots is defined as shown in Figure 5d. For each ink dot that displaces due to deployment of the awns, two dimensions are taken. The first dimension is the distance to the center of the pile. The second dimension is the displacement of the ink dot. If the ink dot undergoes a shape change during the test, the location of the center of the dot is approximated and used as the final position of the ink dot. The ink dots that are displaced lower than the minimum threshold are not considered within the shear plane. Then, for all eight sections of the image, the distances to the center of the pile for the two ink dots that are furthest from the center of the pile are averaged and a radius for the shear plane for that section is determined. The distances for two dots are averaged rather than using one ink dot distance to compensate for human error when defining the displacement distances, as they are manually entered as inputs for the Grasshopper code. Finally, the eight radius values are grouped and averaged to determine the 4 shear plane radius values depicted in Figure 5e. The shear plane radius values r1 and r2 result from the deployment of one awn, and the radius values r3 and r4 result from the deployment of the second awn.

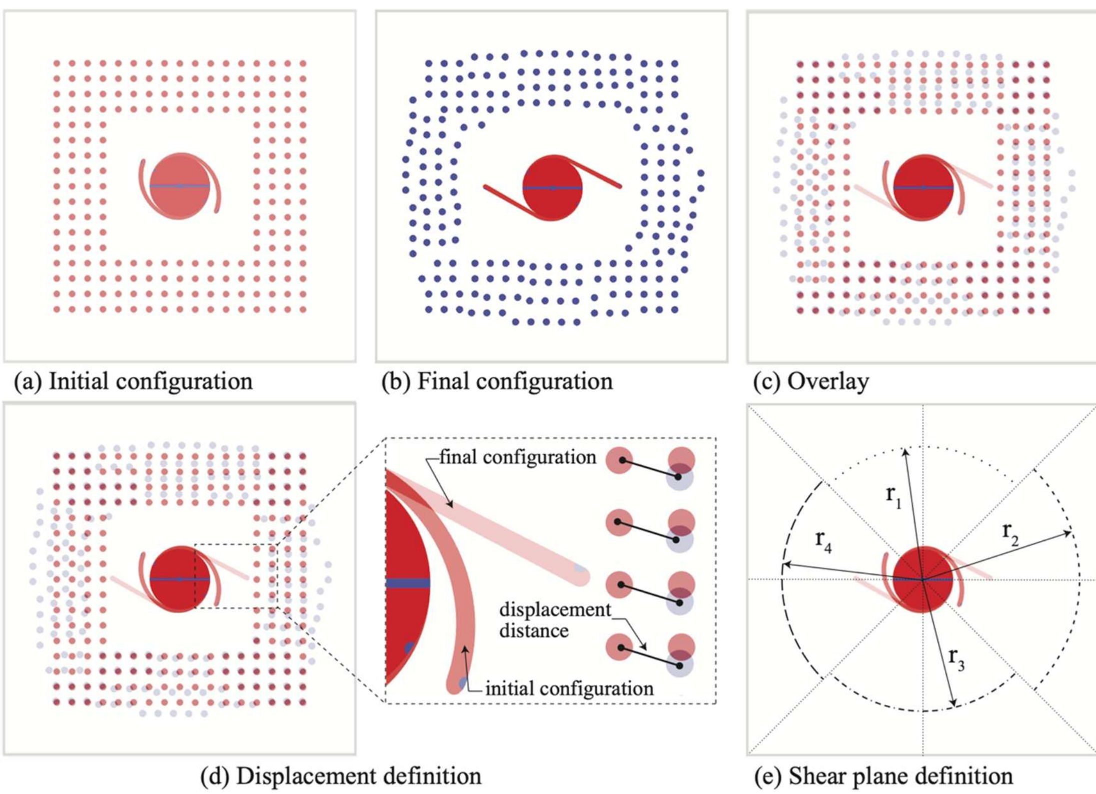

Figure 5. Ink Tracking Technique

3.2 Shear Plane Radius Results

The test procedure and the ink spread tracking technique were completed for three ground anchors of the same geometry, as described in the procedures section. The shear plane radius values for each ground anchor are shown in Table 1, as well as the maximum force applied to deploy the awns, recorded by the force sensor.

Table 1. Shear Plane Radius Results

Test	r_1 (mm)	r_2 (mm)	r_3 (mm)	r_4 (mm)	Maximum Force (N)
1	37.5	48.0	43.6	50.6	7.5
2	43.3	52.1	44.2	52.7	12.9
3	35.8	42.2	37.6	35.5	8.8
Average	38.9	47.4	41.8	46.3	

The results show that the r_1 and r_3 radius values have average values that are smaller than the average values for the r_2 and r_4 radius values. A paired t-test was performed to test the hypothesis that there is no significant difference between the r_1 and r_3 radius values. The t-test proved this hypothesis as the results showed that the t-critical value is 4.3 and the t-value is 0.4996. Similarly, a second paired t-test was completed to test the hypothesis that there is no significant difference between the r_2 and r_4 radius values, and this t-test also proved this hypothesis. The t-critical value is 4.3 and the t-value is 1.83.

A third paired t-test was performed between the larger radius values (r_2 and r_4) and the smaller values (r_1 and r_3) to test the hypothesis that there is a significant difference between these values. The t-test found that there is a statistical difference between the larger values and the smaller values. The t-critical value is 2.57 and the t-value is 3.59. There is 95% confidence that the mean difference between the larger radius values and the smaller radius values is between 1.85 mm and 11.16 mm. This t-test analysis shows that the 180-degree deployment of the ground anchors in sandy soil results in one short radius value and one long radius value for each awn of the ground anchor. For Test 3, the r_4 value is smaller than the r_3 value, and this is the only pair of radius values where this occurs. This discrepancy in results can be attributed to the fact that the 3D printed material does not perform consistently after testing one time.

The maximum force for each test is also reported in Table 1. The maximum applied force to deploy the ground anchors ranges from 7.5 N to 12.9 N. The largest force, 12.9 N, correlates with the largest shear plane radius value, but there are not enough data points to conclude that there is a causational relationship between the applied force and the shear plane radius. Previous experiments in this lab have determined that the maximum force required to deploy a ground anchor of this shape is 20.8 N, which is much larger than the maximum forces found during these tests. Previous experiments used a mixture of sand and sugar water to achieve a translucent sand, and this translucent sand is more cohesive than the sand used in this experiment, and therefore a larger force was needed to deploy the awns.

3.3 Bar and Hinge Model Results

Previous work in this lab determined that the maximum force for deploying one awn in the translucent sand mixture is 12.2 N. This value was used as the applied force in the finite element analysis model to find the in-plane and out-of-plane deformations of the awn. The deformations resulting from this analysis are shown in Table 2. The in-plane and out-of-plane deformations are depicted in Figure 5a and 5b, respectively.

Table 2. Finite Element Analysis Awns Deformations Result

Test	Arc Length (mm)	Height (mm)	Thickness (mm)	Material	Force (N)	Deformation (mm)
Out-of-plane	25	25	2	Vero	12.2	0.0031
In-plane	25	25	2	Vero	12.2	0.1269

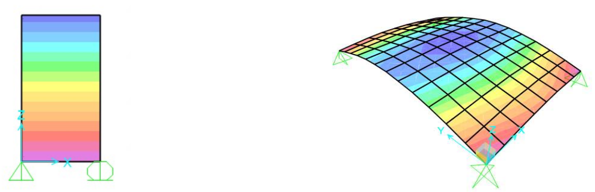

(a) In-plane deformation (b) Out-of-plane deformation

Figure 5. Awn deformation representation for (a) in-plane and (b) out-of-plane deformation using SAP2000 for validation with the bar-and-hinge model

To develop an efficient bar and hinge model capable of accurately predicting these deformations, an iterative approach was undertaken. The diameter values of the bar elements were varied until the resulting deformations of the bar and hinge model fell within 90% accuracy of the finite element model predictions, as described by the methodology in the procedures section. The final bar diameter results are summarized in Table 3.

Table 3. Optimized Bar and Hinge Model Dimensions and Deformations

Test	Vertical Bar Diameter (mm)	Horizontal Bar Diameter (mm)	Cross Bar Diameter (mm)	Deformation (mm)	Accuracy (%)
Out-of-plane	4.50	4.50	3.10	0.0033	93.9
In-plane	4.50	4.50	3.10	0.1202	94.7

The vertical, horizontal, and cross bar diameters can be presented as a ratio between the diameter of the vertical and horizontal bars and the cross bars. These optimal diameter ratios indicate that for an awn with a square shape, the ratio between the vertical and the horizontal bars, and the diagonal bars should be 1.45:1. This ratio serves as a valuable guideline for modeling the square-shaped awns and can be applied to any awn shape with a square size, enabling scaled modeling of multi-awn pile systems constructed from the same material in future studies.

To validate the accuracy of the bar and hinge model, the deformations obtained through the iterative modeling process were compared against the finite element model predictions. Table 4 presents a side-by-side comparison of the maximum in-plane and out-of-plane deformations calculated by both methods.

Table 4. Comparison of Deformations: Finite Element Model vs Bar and Hinge Model

Test	Finite Element Model Deformation (mm)	Bar and Hinge Model Deformation (mm)	Difference (%)
Out-of-plane	0.0031	0.0033	6.1
In-plane	0.1269	0.1202	5.3

The results demonstrate that the bar and hinge model deflections are in close agreement with the finite element analysis, differing by only 5.3% for in-plane deformations and 6.1% for out-of-plane deformations. These relatively small percentage differences validate the assumptions and simplifications inherent to the bar and hinge modeling technique. For any cases where the deflections fall outside the targeted range in future studies, the bar dimensions can be further adjusted through additional iterations of the modeling process to improve accuracy.

4. Conclusions

The ink tracking technique presented in this paper is an effective method for experimentally determining the location of the shear plane in sandy soil from the deployment of the awns of the ground anchor systems. In addition, the equivalent bar area for the thick origami in the bar-and-hinge model was successful in characterizing the in-plane and out-of-plane behavior of the deployable awns. These understandings of how to experimentally analyze and computationally replicate the behavior of the deployable ground anchors are useful techniques that can help in the development of future designs of the deployable anchors.

Acknowledgments

Feel free to acknowledge any sponsors or other individuals. Don’t forget to place standard disclaimers as required by funding agencies.

5. References

Aubeny, C. (2017). *Geomechanics of marine anchors*. CRC Press.

Baruah, A. C., & Sychterz, A. C. (2022). Assessment and Comparison of Cable-Actuation of Pill Bug Inspired Adaptive Origami Structure Using Computer Vision and Dynamic Relaxation. *Frontiers in Built Environment*, *8*, 813543.

Colaço, A., Costa, P. A., Parente, C. M. A., & Cardoso, A. S. (2021). Ground-borne noise and vibrations in buildings induced by pile driving: An integrated approach. *Applied Acoustics*, *179*, 108059.

Filipov, E. T., Liu, K., Tachi, T., Schenk, M., & Paulino, G. H. (2017). Bar and hinge models for scalable analysis of origami. *International Journal of Solids and Structures*, *124*, 26-45.

Kempfert, H. G., & Gebreselassie, B. (1999, July). Effect of anchor installation on settlement of nearby structures in soft soils. In *Proceedings international symposium On Geotechnical Aspects of Underground Construction in Soft Ground, IS-Tokyo* (Vol. 99, pp. 19-21).

Lande, E. J., Karlsrud, K., Langford, J., & Nordal, S. (2020). Effects of drilling for tieback anchors on surrounding ground: Results from field tests. *Journal of Geotechnical and Geoenvironmental*

Engineering, *146*(8), 05020007.
Lawrence, P. L. (1994). Natural hazards of shoreline bluff erosion: a case study of Horizon View, Lake Huron. *Geomorphology*, *10*(1-4), 65-81.
Levine, K. J., Jahn, N. T., Kotz, E., & Roscizewski, A. (2020). What do our lakes mean to us? An understanding of Michigan coastline communities' perceptions of the Great Lakes. *Journal of Great Lakes Research*, *46*(6), 1716-1725.
Lutenegger, A. J., & Tsuha, C. D. H. (2015, December). Evaluating installation disturbance from helical piles and anchors using compression and tension tests. In *Proceedings of the 15th Pan-American Conference on Soil Mechanics and Geotechnical Engineering, Buenos Aires, Argentina* (pp. 373-381). Press.
Poulos, H. G. (1995). Design of reinforcing piles to increase slope stability. *Canadian Geotechnical Journal*, *32*(5), 808-818.
Sakr, M., Nazir, A., Azzam, W., & Sallam, A. (2020). Model study of single pile with wings under uplift loads. *Applied Ocean Research*, *100*, 102187.
Sychterz, A. C., & Baruah, A. C. (2021). Active control for adaptive origami structures undergoing damage. *Engineering Structures*, *242*, 112457.
Tucker, K. A., & Sychterz, A. C. (2022, May). Analyzing Geosystems with Deployable Compliant Mechanisms for Enhanced Tension Capacity. In *Canadian Society of Civil Engineering Annual Conference* (pp. 483-494). Cham: Springer Nature Switzerland.
Volpano, C. A., Zoet, L. K., Rawling III, J. E., Theuerkauf, E. J., & Krueger, R. (2020). Three-dimensional bluff evolution in response to seasonal fluctuations in Great Lakes water levels. *Journal of Great Lakes Research*, *46*(6), 1533-1543.
Wilde, B., Treu, H., & Fulton, T. (2001, June). Field testing of suction embedded plate anchors. In *ISOPE International Ocean and Polar Engineering Conference* (pp. ISOPE-I). ISOPE.